CONCRETE RESEARCH LETTERS

www.crl.issres.net Vol. 3 (4) – December 2012

Shear Strengthening of Self-Compacting Reinforced Concrete Deep Beams With External Bonded Layers

Khaled M. Heiza*, N. N. Meleka and N. Y. Elwkad

Civil Engineering Department, Faculty of Engineering
Menoufiya University, EGYPT

Abstract

Self-compacting concrete (SCC) is a stable and highly flowable concrete. In this study, a new shear strengthening technique for reinforced self-compacting concrete (RSCC) deep beams was suggested and compared with some traditional techniques. An experimental test program consists of sixteen specimens of RSCC deep beams strengthened by different materials such as steel, glass and carbon fiber reinforced polymers (GFRP and CFRP) was executed. Externally bonded layers (EBL) and near surface mounted reinforcement (NSMR) were used as two different techniques. The effects of the new technique which depends on using intertwined roving NSM GFRP rods saturated with epoxy were compared with the other models. The new technique for shear strengthening increases the load capacity from 36% to 55% depending on the anchorage length of GFRP rods. Two dimensional nonlinear isoperimetric degenerated layered finite elements (FE) analysis was used to represent the SCC, reinforcement and strengthening layers of the tested models. The analytical results have been very close to the experimental results.

Keywords: Deep beams, Self-compacting concrete, Near surface mounted, External bonded layers.

1. Introduction

Reinforced concrete (RC) deep beams were often used and encountered in many structural applications such as diaphragms, bridges, water tanks, precast and prestressed construction, foundations, silos, bunkers, offshore structures and tall buildings [1.2].

Many experimental studies have been performed to investigate the behavioral characteristics and the cause of the shear failure of RC beams [3-5]. Several researchers [6.7] and the current codes [8-10] have recommended the design of deep beams using the strut-and tie model. In these strut-and-tie models, the main function of shear reinforcement is to restrain diagonal cracks near the ends of bottle-shaped struts and to give some ductility to struts.

[1*]Corresponding Author, Associate Professor, Civil Engineering Department,
E-mail: khheiza@ yahoo.com, khheiza@ hotmail.com.

Thin deep girders often contain congested shear reinforcement within the web, the normal concrete often does not flow well when traveling through the web, and does not completely fill the bottom bulb. This results in voids in the concrete finish, which often termed bug holes or a honeycombing effect in the finished concrete surface. In this case many researches recommended the use of self-consolidating concrete (SCC) [11-13]. Self-consolidating concrete, also known as self-compacting concrete, yields distinct advantages over typical concrete due to its liquid nature such as: (a) Low noise-level in construction sites, (b) Eliminated problems associated with vibration, (c) Less labor involved, (d) Faster construction, (e) Improved quality and durability, (f) higher strength. In Egypt, SCC is beginning to gain interest, especially for the precast concrete, prestressed concrete and cast-in place construction [14]. Self-consolidating concrete was first developed in 1988 by Okamura [15] to achieve durable concrete structures. Since then, various investigations have been carried out and this type of concrete has been used in practical design method in different countries, mainly by large construction companies. Japan has used SCC in bridge, building and tunnel construction since the early 1990.s. A number of SCC bridges have been constructed in Europe [15.16] and United States [17]. However, SCC is heavy used in precast and prestressed concrete industry [18.19].

Although SCC is a material of the future, it does not come without some disadvantages. SCC is typically made with smaller coarse aggregate sizes and a larger amount of fine materials. This may lead a higher shrinkage values and also can negatively affect the tensile strength and shear strength of the concrete [20].

Increasing the shear strength of Reinforced self-compacting concrete RSCC deep beams may be required in many cases such as changing of building use, the need to perform an opening in deep beams for air conditioning, corrosion of reinforcement and finally due to construction or design errors. A very limited amount of experimental data exists on strengthening of RC deep beams in shear [22]. Strengthening using advanced composite materials such as fiber-reinforced polymer (FRP) rods, strips or woven wraps are being increasingly recognized for enhancing flexural and shear strength of concrete members instead of the traditional materials represented by steel bars or strips [21.22]. Repair and strengthening of structural members with composite materials, such as carbon, glass, kevlar and aramid fiber-reinforced polymers, have recently received great attention [23.24]. Reduced material costs, coupled with labor savings inherent with its lightweight and comparatively simple installation, its high tensile strength, low relaxation, and immunity to corrosion, have made FRP an attractive alternative to traditional retrofitting techniques. Field applications over the last years have shown excellent performance and durability of FRP-retrofitted structures [23.24]. Nowadays, carbon and glass fiber strips, rods and wraps woven in one or multi-directions are widely used as strengthening materials.

Many researchers used FRP for strengthening the flexure strength of beams. Several studies investigated the use of externally bonded FRP composites [21.23] or near surface mounted reinforcement (NSMR) [25-29] to improve the strength and stiffness of RC members.

This paper investigated a series of test specimens consisted of sixteen test specimens. this research has been conducted to assess and compare the ability and efficiency of traditional materials represented by steel bars, strips or plates, as well as advanced composite materials (ACM) represented by GFRP and CFRP woven wraps for shear strengthening of RSCC deep beams with a central opening. The behavior and the results of the tested beams were presented, discussed and analyzed in illustrated figures for the purpose of comparison.

A numerical analysis for modelling the method of strengthening of RSCC deep beams was developed and a computer program was prepared to model such case study. This paper explains the method of analysis using 2-D nonlinear isoperimetric degenerated layered finite elements with eight nodes and five degrees of freedom at each node. The layered technique was used to represent the SCC, steel reinforcement and the different strengthening layers of the tested deep beams. The proposed FE model results have been verified and compared by the experimental test results.

Research Objectives

The main objective of this research is to determine the improvement of the shear strength of RSCC deep beams using a new innovative technique. This technique is applied using NSM GFRP rods manufactured from intertwined GFRP roving saturated with epoxy resin in vertical and inclined directions at both sides of the beam surfaces. These rods were anchored through the thickness of the beam web in transverse direction. The new method of strengthening was compared with some other common techniques such as external bonded layers of steel and FRP wraps as well as with NSMR using steel strips and bars as well as CFRP strips and wraps in order to insure the effectiveness of the new developed method.

The goal of this research is extended to introduce a new model for the nonlinear FE method using a high performance iso-parametric degenerated layered element to represent all the composite materials such as SCC, reinforcement, and strengthening layers. The FE model will be interpreted to a developed computer program to ease the analysis of many cases with other boundary conditions or material characteristics. The results of the numerical program will be verified by the experimental results.

2. Experimental Test Program

An experimental test program was carried out to investigate the behavior of RSCC deep beams strengthened using EBL and NSMR techniques. Steel, GFRP and CFRP were used as the main strengthening materials.

The experimental program consists of sixteen test specimens that have constant cross section with dimensions of 1200 x 500 mm, and effective span (1000 mm). One specimen without opening and the other fifteen test specimens were cast with a central opening of dimension 200 x 200 mm. Each beam has a lower longitudinal reinforcement 4Φ16 mm as a main flexural reinforcement of high tensile steel, top reinforcement 2Φ10 mm as stirrup hangers, 4Φ6 as side reinforcement and stirrups ϕ6 mm @15 cm of mild steel. Two beams were considered as a reference control beams. One beam without opening identified BR and the other with a central opening identified BOR. Fig. 1 shows the dimensions and the details of reinforcement for the reference beam BOR.

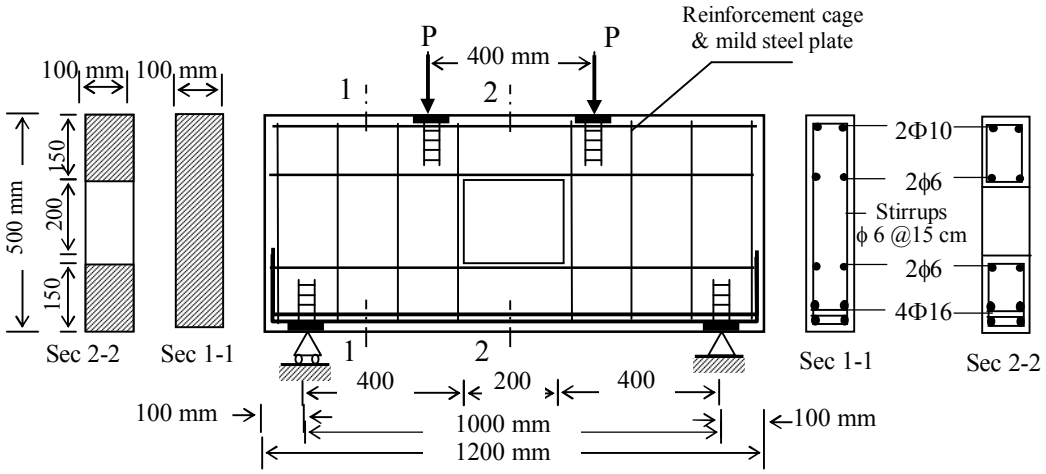

Fig. 1: Typical dimensions and details of reinforcement of the reference beam BOR

3. Materials Properties and Mix Design

SCC can be largely affected by the characteristics of materials and mix proportion. In this research, the mix design of SCC is based on a CIB method [14]. The properties of the materials used in this study were summarized as follows:

Cement: A locally produced ordinary Portland cement complied with E.S.S.373/91 requirements.

Aggregates: The fine aggregates were siliceous natural sand. The coarse aggregates were crushed dolomite with maximum nominal size 14 mm.

Silica fume: is a product resulting from the industry of Ferro-silicon alloys, the product is a rich silicon dioxide powder where the average size is a round 0.1 micrometers [30].

Fly ash: one of the mineral admixtures used in this experimental is fly ash its commercial name is Supper Pozz-5 [30].

Viscosity Enhancing Agent (VEA): is the super-plasticizer used in this experimental the commercial name is Sika- Viscocrete 5-400 from Sika Egypt [**Error! Bookmark not defined.**].

Table 1 gives the chosen mix proportions of materials used for casting the RSCC deep beam models and Table 2 shows the properties of the used reinforcement steel.

Table 1: Mix proportions for casting one cubic meter of SCC [30]

	C (MPa)	W/C (MPa)	F.A (MPa)	C.A (MPa)	S.F. (MPa)	F.A. (MPa)	VEA (MPa)	f_{cu} after 28 days (MPa)
Mix Proportion	1	0.3	2.25	2.25	0.15	0.10	0.025	40

Where: C = Cement with content 400 Kg/m^3, W/C = Water cement ratio, F.A. = Fine aggregate (sand), C.A. = Coarse aggregate (crushed dolomite), S.F. = Silica fume, F.A. = fly ash as a mineral admixture, VEA = Viscosity enhancing agent.

Table 2: Mechanical properties of steel used in the test program [30]

Steel Type	Yield Strength σ_y (MPa)	Tensile Strength σ_u (MPa)	Elongation Δ (%)	Young's Modulus E (MPa)
High tensile	386.5	556.3	15.11	$21x10^4$
Mild steel	265.8	394.5	23.21	$20.5\ x10^4$
Steel plates	255.2	407.8	20	$21x10^4$

4. Strengthening Schemes

Two reference RSCC deep beams labeled BR, BOR were loaded till failure without strengthening. The letter ' R ' stands for reference beam, and the letter ' O' stands for beam with an opening. The other fourteen models were classified into three groups according to the strengthening materials. Three main materials were used for purpose of comparison. Steel bars ϕ 6 mm, steel plates 1 mm and 3 mm thickness were used as traditional materials, while GFRP roving and wraps

as well as CFRP strips and wraps were used as advanced strengthening materials. Two main techniques for shear strengthening were executed. The first by using NSM vertical and inclined reinforcement as shown in Fig. 2, and the second by EBL as shown in Fig. 3. The three groups were summarized as follows:

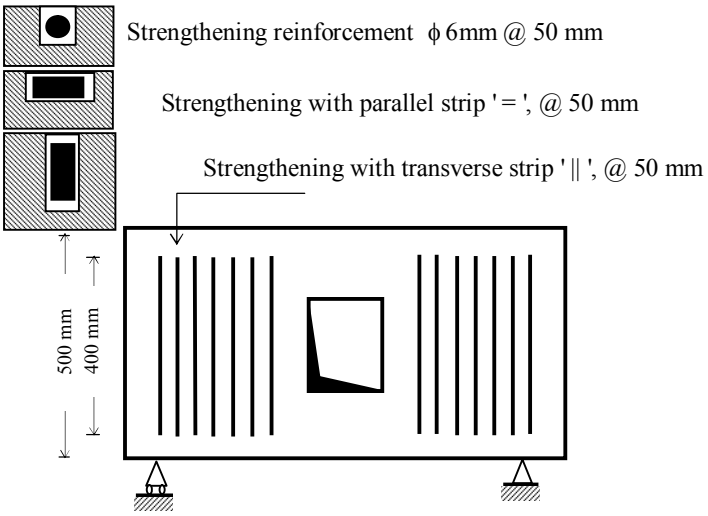

(a) NSM vertical reinforcement
BOVSB, BOVSP=, BOVSP||, BOVSP||3, BOVG1, BOVG2, BOVC=, and BOVC||

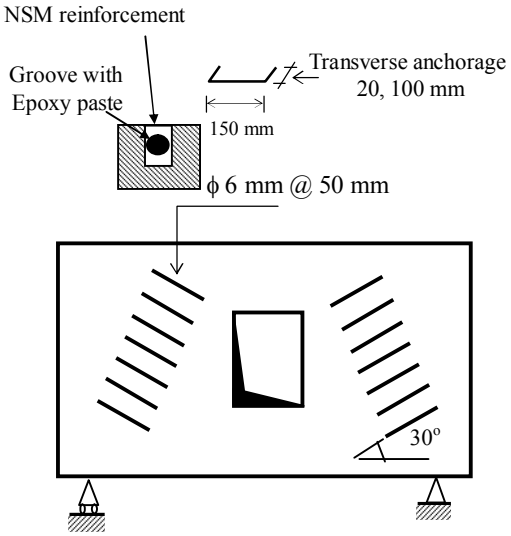

(b) NSM inclined reinforcement (30°) for models BOISB, BOIG1, BOIG2

Fig. 2: Shear strengthening for RSCC deep beams from both sides by NSMR

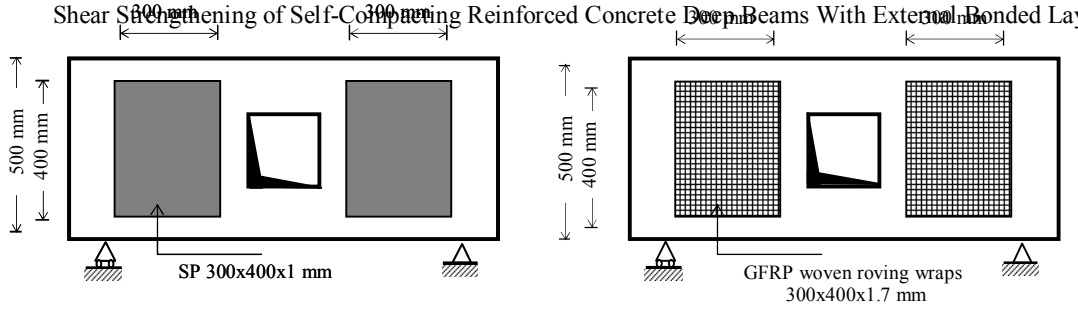

(a) EBL steel plates, BOSPL (b) EBL GFRP woven wraps, BOGW

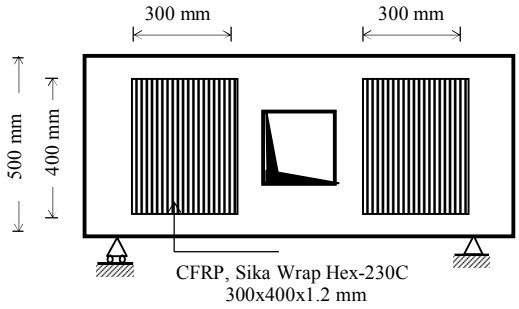

(c) EBL CFRP wraps, BOCW

Fig. 3: Shear strengthening by externally bonded additional layers

4.1 Group (A)

Group (A) contains six models strengthened by steel; BOVSB, BOVSP=, BOVSP||, BOVSP||3, BOISB and BOSPL. The letter ' V ' stands for vertical strengthening, and 'I' for inclined strengthening, while the letters ' SB ' stands for steel bars, and ' SP ' for steel plates. The symbol ' = ' indicates that the long side of the cross section of the strip is parallel to the surface of the beam, while the symbol ' || ' points to strengthening with strips in transverse direction to the surface, and ' 3 ' refers to strengthening with steel strips 3mm thickness. ' L' indicates for strengthening by steel plates as external layers.

4.2 Group (B)

Group (B) consists of five models strengthened with NSM vertical and inclined GFRP intertwined rods manufactured manually from E-glass roving embedded in epoxy resin as a new technique, and also with GFRP woven wraps as EBL (Figs.2 and 3). The five models are BOIG1, BOIG2, BOVG1, BOVG2, and BOGW. The letter 'G' stands for strengthening by GFRP, and (1, 2) indicate two different cases of anchored length 20mm and 100mm through the beam web in transverse direction respectively. The letter 'W' stands for strengthening by FRP woven wraps.

4.3 Group (C)

Group (C) comprises three models strengthened with CFRP; BOVC=, BOVC||, and BOCW. The letter 'C' stands for strengthening by CFRP.

Figure 2 and 3 show the different shear strengthening by NSMR and EBL techniques respectively. In NSMR, a groove was cut in the desired direction throughout the concrete surface. The size of the groove was made to allow for clearance around the rod as shown in Fig.4. The rut

was then filled halfway with epoxy paste, the strengthening reinforcement was placed in its position and lightly pressed. To force the paste to flow around the rod and fill completely any space between the rod and the sides of the groove. The groove was then filled with more paste and the surface was leveled. Steel bars and plates, GFRP intertwined rods manufactured manually from E-Glass Roving and epoxy resin [30] as showed in fig. 5 as well as CFRP strips were used as NSMR.

In the second technique, additional external bonded layers were then bonded to the concrete surfaces of the RSCC model using epoxy resin. Steel plates, GFRP woven wraps in two perpendicular directions and also CFRP woven wraps in uni-direction were used. Different types of FRP used in this research are showed in Fig. 6.

Table 3 shows the properties of FRP strengthening materials used in this research work.

Table 4 summarizes the experimental test program and specifies the RSCC deep beams in different groups

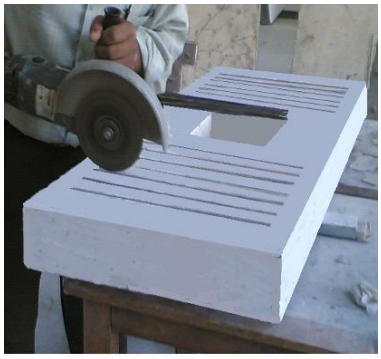

Fig. 4: Grooves were cut in the desired direction for NSMR

Fig. 5: NSM intertwined rods were stitched through the beam

(a) GFRP Woven Roving wraps

(b) E-Glass-Roving

(c) Sika Wrap Hex -230C

(d) Strips of Sika CarboDur – S1012

Fig. 6: Different FRP used for strengthening RSCC deep beams

Table 3: Mechanical properties of GFRP and CFRP used in the test program [30]

Property	E-GLASS Woven Roving Wraps (WR)	Sika Wrap Hex-230C	CFRP Plates Sika CarboDur – S1012
Fabric thickness, cm	0.17	0.12	0.12
Tensile strength, σ MPa	290	4100	3050
Modulus of elasticity, E MPa	13250	230000	165000
Elongation %	2.0	1.7	1.7

Table 4: Experimental test program of strengthened RSCC deep beams [30]

Group	Specimen code	Dimensions of applied material (mm)	Shear strengthening method
Reference Beams	**BR**	-	Reference RSCC beam without openings was loaded up to failure, P_f without strengthening.
	BOR	-	Reference beam with a central opening was loaded up to failure, P_f without strengthening (Fig.1)
Group (A) Strengthening by steel	**BOVSB**	Steel bars, ϕ 6, L= 400 Anchorage=20mm	Strengthened by NSM vertical steel bars in both sides of the beam (Fig. 2a).
	BOVSP=	Steel plates, 400x10x1	Strengthened by NSM vertical steel strips parallel to the surface in both sides of the beam (Fig. 2a).
	BOVSP‖	Steel plates 400x10x1	Strengthened by NSM vertical steel strips transverse to the surface in both sides of the beam (Fig. 2a).
	BOVSP‖3	Steel plates 400x10x3	Strengthened by NSM vertical steel strips transverse to the surface in both sides of the beam (Fig. 2a).
	BOISB	Steel bars ϕ 6 , L=150	Strengthened by NSM inclined steel bars in both sides of the beam (Fig. 2b).
	BOSPL	Steel plates 400x300x1	Strengthened by externally bonded steel plates by epoxy in both sides of the beam (Fig. 3a).
Group (B) Strengthened by GFRP	**BOVG1**	GFRP rods, ϕ 6, L= 400 Anchorage=20	Strengthened by NSM vertical intertwined rods manufactured from GFRP roving and epoxy in both sides of the beam (Fig. 2a) with an anchorage length equals 20 mm through the web.
	BOVG2	GFRP rods, ϕ 6, L= 400 Anchorage=100	Strengthened by NSM vertical intertwined rods manufactured from GFRP roving and epoxy in both sides of the beam (Fig. 2a) with an anchorage length equals 100 mm through the web.
	BOIG1	GFRP rods, ϕ 6, L=150 Anchorage=20	Strengthened by NSM inclined intertwined rods manufactured from GFRP roving and epoxy in both sides of the beam (Fig. 2b) with anchorage length equals 20 mm through the web.
	BOIG2	GFRP rods, ϕ 6 , L=150 Anchorage=100	Strengthened by NSM inclined intertwined rods manufactured from GFRP roving and epoxy in both sides of the beam (Fig. 2b) with anchorage length equals 100 mm through the web.
	BOGW	GFRP wraps, 400x300x1.7	Strengthened with one layer of externally bonded GFRP woven wraps by epoxy in both sides of the beam (Fig. 3b).
Group © Strengthened by CFRP	**BOVC=**	CFRP plates 400x10x1.2	Strengthened by NSM vertical CFRP strips parallel to the surface in both sides of the beam (Fig. 2a).
	BOVC‖	CFRP plates 400x10x1.2	Strengthened by NSM vertical CFRP strips transverse to the surface in both sides of the beam (Fig. 2a).
	BOCW	CFRP wraps 400x300x1.2	Strengthened by one layer of externally bonded CFRP wraps by epoxy in both sides of the beam (Fig. 3c).

Where: is the length of NSM reinforcement.

5. Test Set-Up and Instrumentation

The reference beams were loaded up to failure without strengthening while the other beams were loaded after strengthening up to failure. Models were tested under two concentrated loads. A steel frame of 200 ton capacity was used for testing beams in RC laboratory Collage of Engineering, Menoufiya University, Egypt. Loads were applied in increments using a hydraulic jack of 100 ton maximum capacity as shown in Fig. 7. Dial gauges of 0.01 mm accuracy and a total capacity of 25 mm were fixed to measure the deflection at mid-span, under the two concentrated loads and at 100 mm form the end supports. Demec points were arranged and fixed on the painted side of each tested beam near top and bottom surfaces of the beam in four rows at the center of span. Concrete strains were measured by mechanical strain gauges of 200 mm gauge length and 0.001 mm accuracy. A magnifying lens was used to observe the crack propagation clearly. Cracks were traced and marked at each load increment. Figure 7 shows the arrangement of dial gauges and demec points.

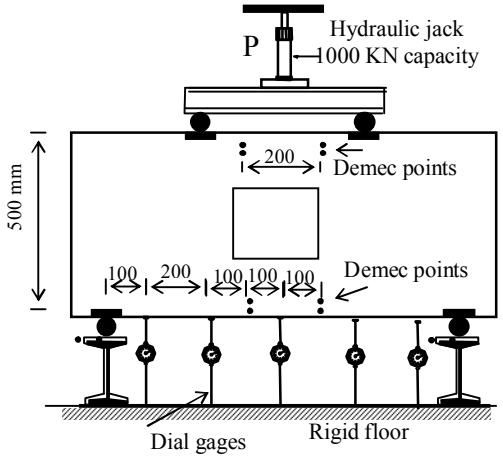

Fig. 7: Test setup and instrumentation

6. Analysis of the Test Results

The different groups of RSCC deep beams were tested. The results were illustrated and compared at different stages of loadings. The load-deflection curves were plotted, the first cracking and failure loads were recorded and compared. The crack propagations were also marked after each load increment and photographed at failure.

6.1 Deflection

Fig. 8 compares the load deflection curves at mid-span for beams strengthened by the new technique using vertical NSM intertwined roving GFRP rods with that strengthened with NSM vertical steel bars. The results were compared also with the reference beam BOR. At the ultimate failure load of BOR, deflections of beams, BOVSB, BOVG1, and BOVG2 were decreased by about 42%, 28%, 31% respectively. Fig. 9 shows the load deflection curves at mid-span for beams strengthened by the new technique using inclined NSM intertwined roving GFRP and the beams strengthened with NSM inclined steel bars. At the ultimate failure load of BOR, deflections of beams, BOISB, BOIG1, and BOIG2 were decreased by about 22%, 19% and 36% respectively. It is clear from Figs 8 and 9 that the new technique using GFRP improves the structural behavior and the reduction of the deflections increases with increasing the anchorage length.

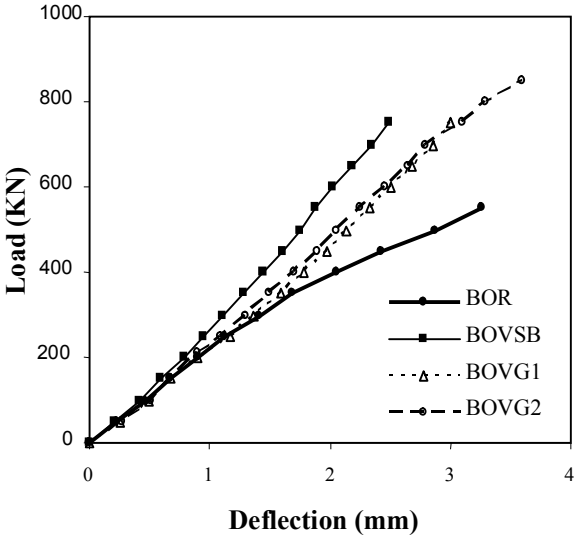

Fig. 8: Load–deflection curves for beams strengthened by vertical NSMR

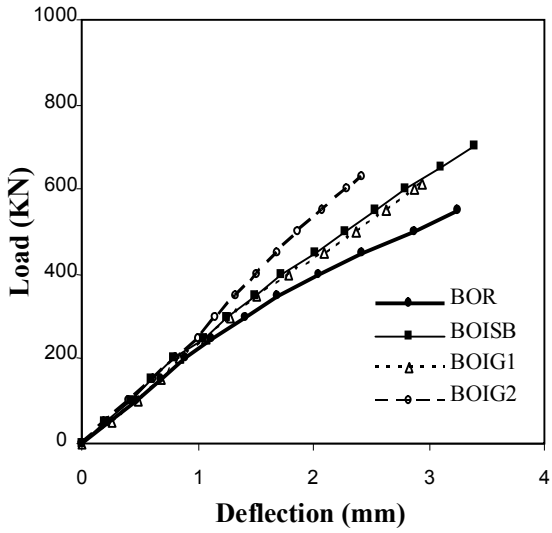

Fig. 9: Load–deflection curves for beams strengthened by inclined NSMR

Fig. 10 compares the load deflection curves at mid-span for beams strengthened by using vertical NSM parallel and transverse strips. At the ultimate failure load of BOR, deflections of beams, BOVSP=, and BOVC= were decreased by about 29% and 39% respectively. Deflections of beams BOVSP||, BPVSP||**3** and BOVC|| were decreased at the same level by about 22%, 42% and 52% respectively. The results of using vertical transverse strips showed better improvement than using the parallel strips. The maximum reduction was recorded by CFRP strips in the transverse direction.

Fig. 11 shows that the use of EBL at both sides of RSCC deep beams improves the structural behavior. At the ultimate failure load of BOR, deflections of beams, BOSPL, BOGW, and BOCW were decreased by about 11%, 20 and 26% respectively.

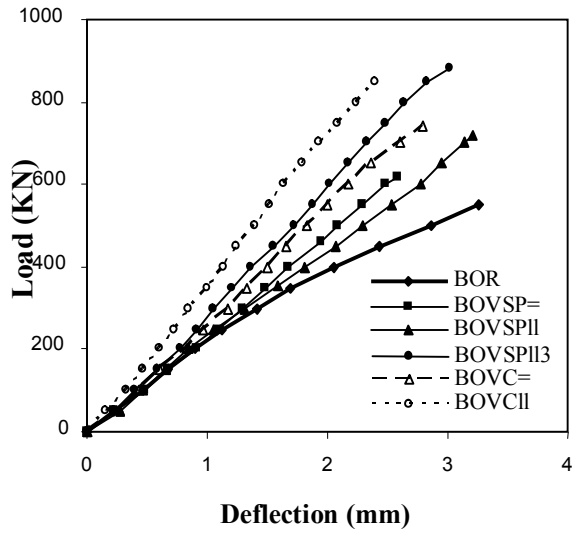

Fig. 10: Load –deflection curves for beams strengthened by vertical NSM strips

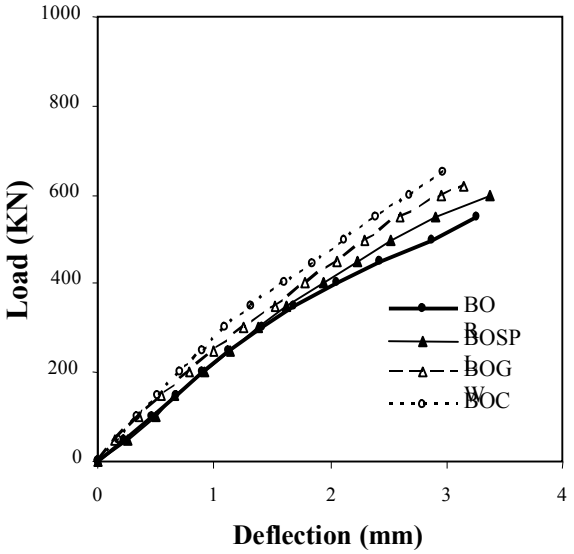

Fig. 11: Load –deflection curves for beams strengthened by EBL

6.2 Cracking and ultimate loads

The first cracking and the ultimate failure loads were recorded for the tested beams. All the tested RSCC deep beam models failed in shear. Fig. 12 compares both cracking and failure loads of the different groups of beams with the reference control beams. It is clear that the ultimate load of the control beam BR was higher than the ultimate load of control beam BOR by about 9%. As compared with the control beam BOR, the increase in the ultimate failure loads in Group (A) recorded for strengthened beams BOVSB, BOISB and BOSPL were about 36 %, 27% and 9% respectively. But the increase were about 13%, 31% and 60% for beams BOVSP=, BOVSP|| and BOVSP||3 respectively. In Group (B), the increase were about 36% and 55% for beams BOVG1 and BOVG2 while they were about 11% and 15% for beam BOIG1 and BOIG2 respectively. In Group C, the capacity of the strengthened beams BOVC=, and BOVC||, were increased by about 35% and 55% of that recorded for BOR respectively.

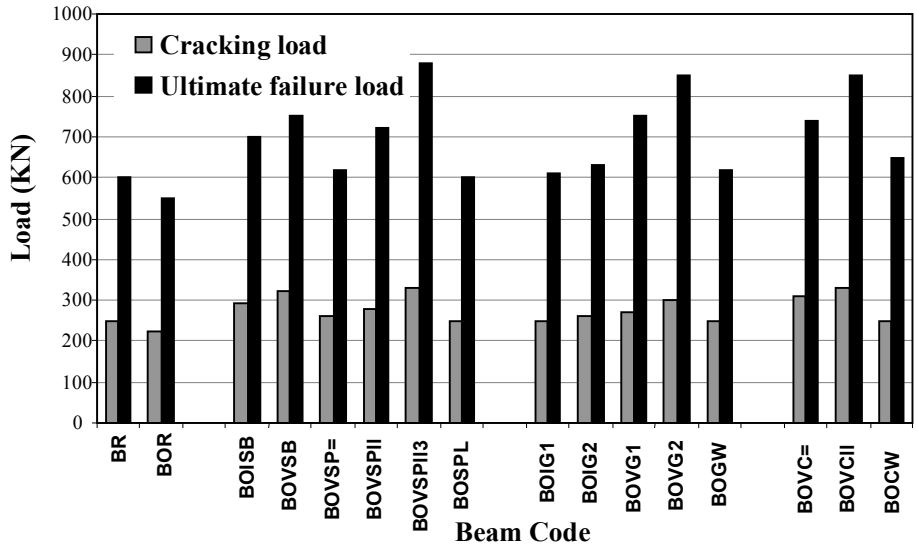

Fig. 12: Comparison between cracking and ultimate loads of RSCC deep beams strengthened with different techniques and materials

It was noticed form the comparison that the new technique which used intertwined roving NSM GFRP rods results in improving the overall structural behavior with respect to the traditional methods. Anchoring the rods with 100 mm drilled through the web in the transverse direction for beam BOVG2, increased the load capacity by about 13% than beam BOVG1 when the anchorage length was only 20 mm. So, it is recommended to increase the anchorage length in the transverse direction to increase the effect of the strengthening process.

The comparison also shows that shear strengthening using NSM CFRP strips in the transverse direction to the face gives the best results of both deflection and ultimate failure loads. It was noticed also that shear strengthening using NSMR increases the ultimate capacity more than the EBL technique with the corresponding material in this case study.

6.3 Cracking Patterns

Figs. 13 and 14 show the crack patterns at different loading stages for beams strengthened by NSM technique. The mode of failure for all illustrated beams was shear failure. It is shown from the figures that the presence of central opening has small effect in case of shear failure.

Fig. 13 shows crack patterns of RSCC deep beams strengthened by inclined reinforcement. It was found that cracks started from the lower level near the center of the beam at the tension side

and developed upward. For further loading, the cracks developed in the region near supports and directed towards the loading position till the failure forming a shear failure. It is noticed from Figs. 13 (a,b) that strengthening bars arrest cracks form developing in the regions of strengthening. Cracks developed around the outer perimeter of the strengthening areas as shown. It is recommended to increase the length of the inclined NSM bars to get better results. Figs. 13 (c, d) show the crack patterns of beams, BOIG1 and BOIG2, strengthened by inclined intertwined roving NSM GFRP rods with anchorage lengths 20 mm and 100 mm respectively. It is shown that increasing the anchorage length of the strengthening bars improves the results and increases the loading capacity.

Fig. 14 shows the crack patterns of RSCC deep beams strengthened by NSM vertical reinforcement. Beam BOVSP||3 had maximum load capacity as shown in Fig. 14 (b). Fig. 4 (c) indicates that using the vertical intertwined roving NSM GFRP rods improves the results. It is noticed from Fig. 14 (d) that shear strengthening with NSM CFRP vertical strips in the transverse direction to the surfaces gives good results.

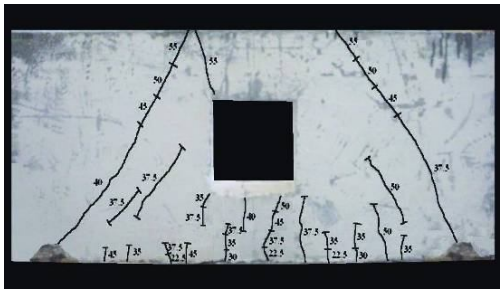

(a) BOR, (P_{ult}= 550 KN)

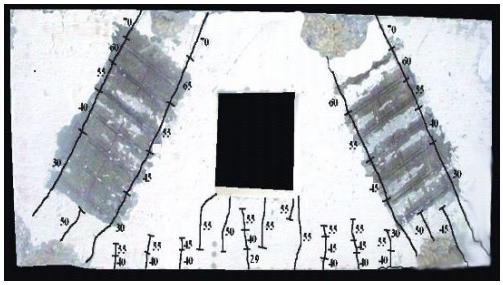

(b) BOISB, (P_{ult}= 700 KN)

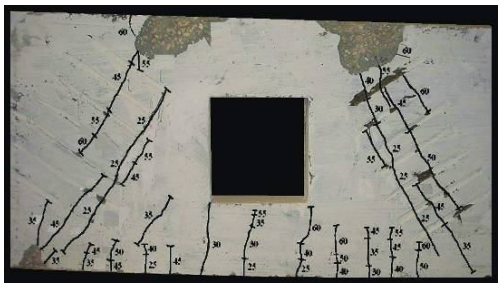

(c) BOIG1, (P_{ult} = 610 KN)

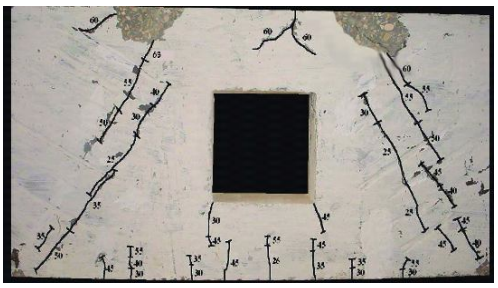

(d) BOIG2, (P_{ult} = 630 KN)

Fig. 13: Crack patterns of RSCC beams strengthened by NSM inclined reinforcement

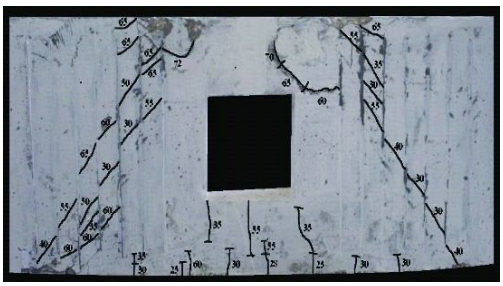

(a) BOVSP||, (P_{ult}= 720 KN)

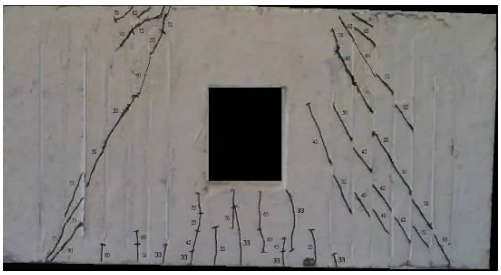

(b) BOVSP||3, (P_{ult}= 880 KN)

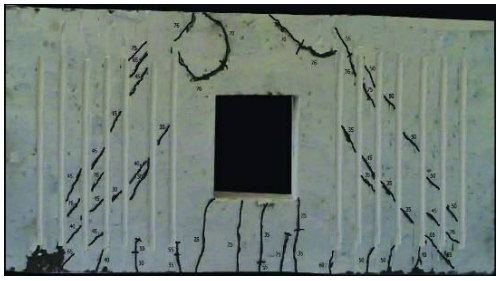

(c) BOVG1, (P_{ult} = 760 KN)

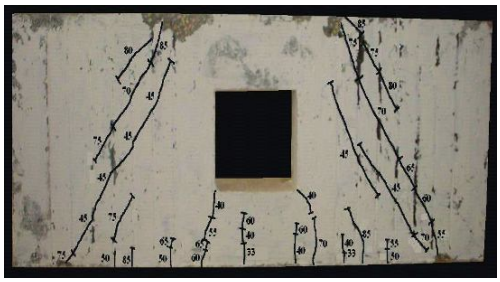

(d) BOVC||, (P_{ult} = 850 KN)

Fig. 14: Crack patterns of RSCC deep beams strengthened by NSM vertical reinforcement

7. Finite Element Analysis

The reinforced concrete beams were modeled in many researches by 3D FE analysis with steel reinforcement as embedded bars [30-34]. SCC reinforced with FRP bars was modeled also by 3D isoparametric elements [35]. In this research, RSCC deep beams were modeled using 2D plane stress isoparametric degenerated layered finite elements. The applied two dimensional elements are degenerated from the three dimensional elements [35]. The main features of the chosen element and the nonlinear procedures will be reviewed briefly.

7.1 Geometric definitions of the element

Transverse shear deformations were considered by applying Reissner-Mindlin plate theory which permits the applications for both thin and thick elements. The finite element has eight nodes. Each node of the element is specified by three coordinates x,y and z for both the top and bottom coordinates of each node to enable the representation of the element in the space. The relation between the Cartesian coordinates of any node and the curvilinear coordinates can be written for 8-node degenerated element as follows:

$$\begin{Bmatrix} x \\ y \\ z \end{Bmatrix} = \sum_{i=1}^{8} N_i(\xi,\eta) \begin{Bmatrix} x_i \\ y_i \\ z_i \end{Bmatrix}_{mid.} + \sum_{i=1}^{8} N_i(\xi,\eta) \frac{\zeta}{2} V_{3i}, \quad (1)$$

Where V_{3i}: is a vector constructed from the nodal coordinates of the top and bottom surfaces at the node i as shown in Fig. 15 (a),

$$V_{3i} = \begin{Bmatrix} x_i \\ y_i \\ z_i \end{Bmatrix}_{top} - \begin{Bmatrix} x_i \\ y_i \\ z_i \end{Bmatrix}_{bottom}, \quad (2)$$

Ni (ξ,η) are the shape functions and ξ, η, ζ are the curvilinear coordinates of the point. The shape functions for the eight boundary nodes are illustrated in Fig. 15 (b) which are serendipity shape functions and defined by the following equations:

(i) For corner nodes (i = 1,3,5,7):

$$N_i = \frac{1}{4}(1+\xi\xi_i)(1+\eta\eta_i)(\xi\xi_i+\eta\eta_i-1). \quad (3)$$

(ii) For mid-side nodes (i = 2, 4, 6, 8):

$$N_i = \frac{\xi_i^2}{2}(1+\xi\xi_i)(1-\eta^2)+\frac{\eta_i^2}{2}(1+\eta\eta_i)(1-\xi^2). \quad (4)$$

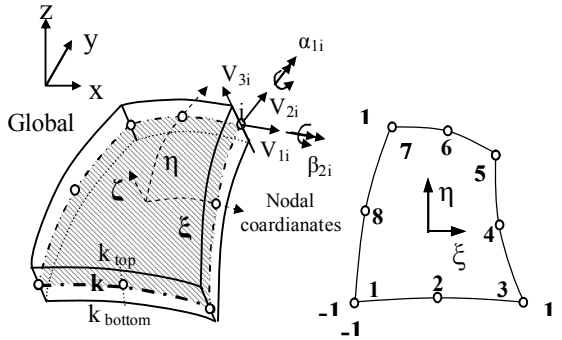

(a) Loacal and global (b) Isoparametric

Fig. 15: Coordinate systems for isoparameteric degenerated element

7.2 Displacements

The displacement field is described by five degrees of freedom; three displacements of the mid-surface node (u, v, w) and two rotations (α_i , β_i) as follows:

$$\begin{Bmatrix} u \\ v \\ w \end{Bmatrix} = \sum_{i=1}^{8} N_i(\xi,\eta) \begin{Bmatrix} u_i \\ v_i \\ w_i \end{Bmatrix}_{mid.} + \sum_{i=1}^{8} N_i(\xi,\eta) \frac{\zeta h_i}{2} [V_{1i} - V_{2i}] \begin{Bmatrix} \alpha_i \\ \beta_i \end{Bmatrix}, \quad (5)$$

Where h_i . is the thickness of the element at the node i

$$V_{1i} = i \times V_{3i}, \qquad V_{2i} = V_{1i} \times V_{3i}, \quad (6)$$

in which i is the unit vector in the x-direction.

7.3 Layered discretization

The FE can be divided into an optional number of concrete, steel, and any additional repair or strengthening layers as shown in Fig.16.

Each layer may have different material properties corresponding to its state of stress. The stresses are computed at the mid-surface of the layer and are assumed to be constant over the thickness of each layer as shown in Fig. 17. Different layer thicknesses can be taken into account as well as different numbers of layers per element.

The layer thickness was defined in terms of curvilinear coordinate ζ to permit the variation of the layer thickness when the element thickness varies. The stiffness of the element $\underline{K}^e$ is obtained by numerical integration through the thickness:

$$\underline{k}^e = \iiint \underline{B}^T \underline{D} \underline{B} J d\zeta d\xi d\eta, \quad (7)$$

$$\underline{f}^e = \iiint \underline{B}^T \sigma J d\zeta d\xi d\eta, \quad (8)$$

where: $\underline{B}$ is the strain matrix composed of derivatives of the shape functions and J is the determinant of the Jacobian matrix.

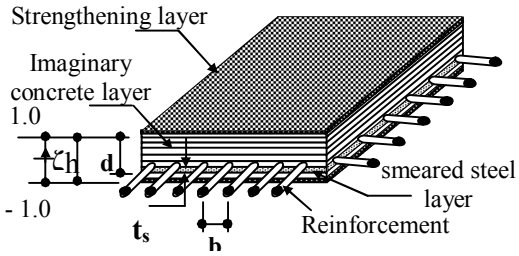

Fig. 16: RSCC element with strengthening layers

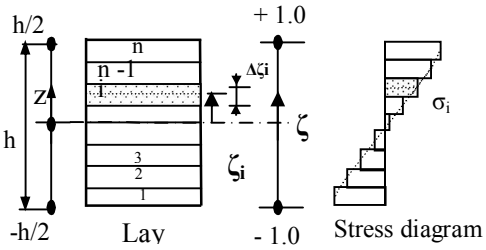

Fig. 17: Layered element; curvlinear coardinate and stress diagram

8. Nonlinear Constitutive Model

The FE technique permits more realistic analysis for reinforced concrete complexities which arise from concrete cracking, tension stiffening, nonlinear multi-axial material properties and complex interface behavior. In the present study, both the perfect and the strain-hardening plasticity approach are considered to model the compressive behavior of the concrete. The flow theory of plasticity [36] is employed to establish the nonlinear stress-strain relations in the plastic range. The assumed yield criterion used in this analysis depends on the Kupfer's results and can be defined as follows:

$$f(\sigma) = \left\{1.355[(\sigma_x^{\,2} + \sigma_y^{\,2} - \sigma_x\sigma_y) + 3(\tau_{xy^2} + \tau_{xz}^{\,2} + \tau_{yz^2})] + 0.335\sigma_o(\sigma_x + \sigma_y)\right\}^2 = \sigma_o. \quad (9)$$

The yielding criteria of this expression as well as Kupfer's results and Von-Mises assumptions are compared in Fig. 18.

The tension stiffening effect is considered by assuming a gradual release of the concrete stress component normal to the cracked plane [36] as shown in Fig. 19. The modulus of elasticity is decreased as the strain increases due to cracking following the next formula:

$$E_i = \frac{\alpha f_t^{'}}{\varepsilon_i}\left(1 - \frac{\varepsilon_i}{\varepsilon_m}\right); \varepsilon_t \le \varepsilon_i \le \varepsilon_m \quad (10)$$

Where: f_t' is the modulus of rupture of the concrete and α, ε_m are tension stiffening parameters.

Shear retention factors can strongly influence a nonlinear solution, especially if shear is prominent as the case of deep beams [37]. To achieve the aim of incorporating a realistic shear

retention factors in order to model shear transfer across cracked concrete, a quadratic function is used [38-40] based on the assumption of direct strain normal to the crack.

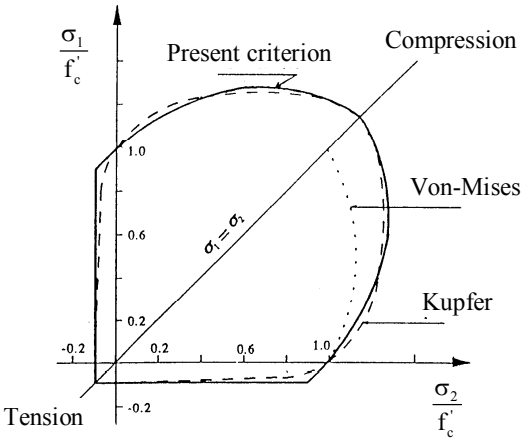

Fig .18 : Yield criterion for concrete

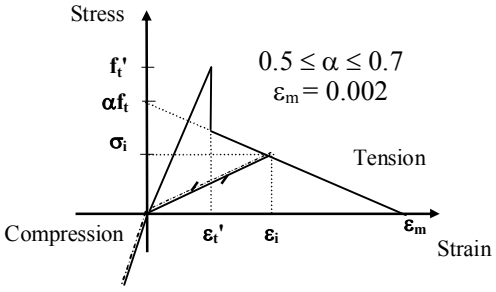

Fig.19 Tension stiffening model

8.1 Reinforcement and strengthening layers

The properties of the strengthening materials of bars, strips, or wraps are generally well defined. Each strengthening layer has an uniaxial behavior, resisting only axial forces in the bar or fiber direction.

In this research reinforcing or strengthening bars are replaced by equivalent smeared distributed lamina. The equivalent thickness of the lamina is considered as follows:

$$t_s = \frac{A_\phi}{b} = \mu \times d, \qquad (11)$$

Where A_ϕ is the cross-sectional area of one bar, b is the spacing between bars, μ is the reinforcement ratio and d is the effective depth of the element. The thickness of the strengthening layer and the effective depth are specified in the analyses by the curvilinear coordinate ζ. The orthotropic layer can be assumed to be isotropic in plane 1. If the lamina principal axes (1,2) do not coincide with the reference axes (x,y) but are at some arbitrary orientation θ to them as shown in Fig. 20, the constitutive relationship for each individual lamina are transformed to the reference axes. In the analysis, smeared layers are assumed to be fully bonded with concrete.

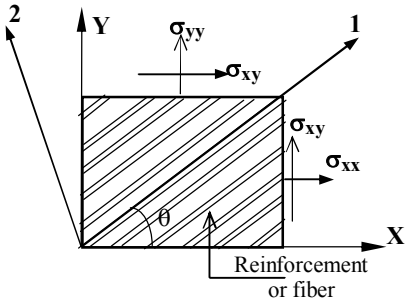

Fig.20: Orientation of orthotropic lamina about reference axes

8.2 verification of the FE model

The previous proposed FE model is performed for the analysis of RSCC deep beams strengthened with inclined and vertical NSM reinforcement for GFRP intertwined roving rods. Figs. 21 and 22 show the FE meshes for the analysis of both vertical and inclined strengthening.

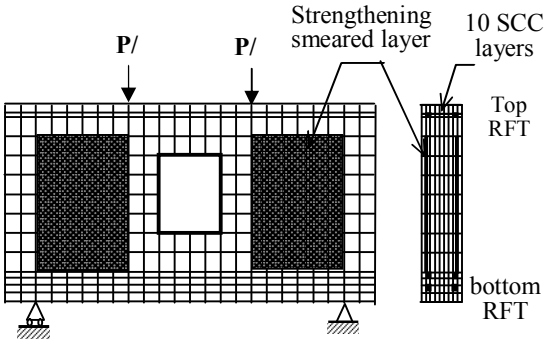

Fig. 21: Finite element mesh for beams BOVSP and BOVG2

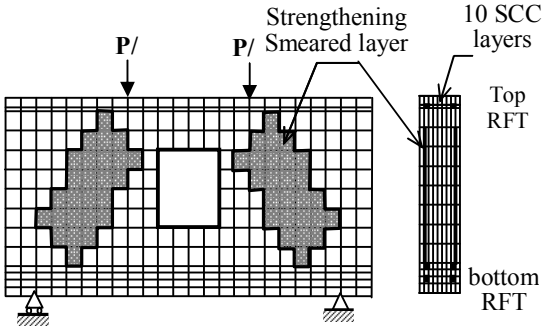

Fig. 22: Finite element mesh for beams BOISP and BOIG2

Fig. 23 compares the load deflection curves for the experimental and numerical results of the beam models BOR, BOVG2, and BOIG2. The FE results showed a good agreement with the experimental test results at different loading stages. At failure loads, the deflections by FE of beams BOR, BOVG2, and BOIG2 were decreased by about 11%, 12.5% and 11.5% respectively.

Fig. 24 compares the ultimate loads of the investigated beams for both experimental and analytical results. The numerical results gave small increases than the experimental results. Specimens BOR, BOVG2, and BOIG2 showed differences of 9%, 12% and 11 %, respectively. It can be observed that the suggested FE model is quite accurate in representing the problem and can be used to study different cases of strengthened specimens that are not included in the experimental program.

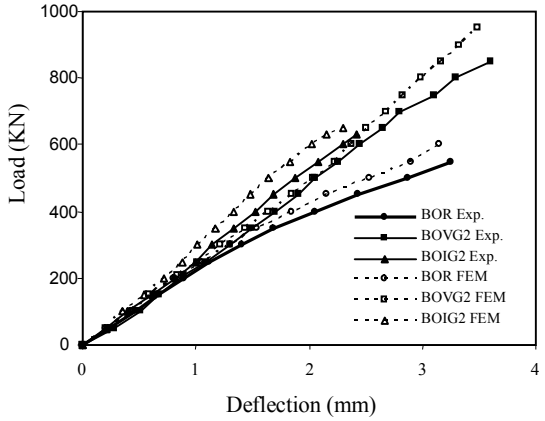

Fig. 23: Experimental and analytical load deflection curves

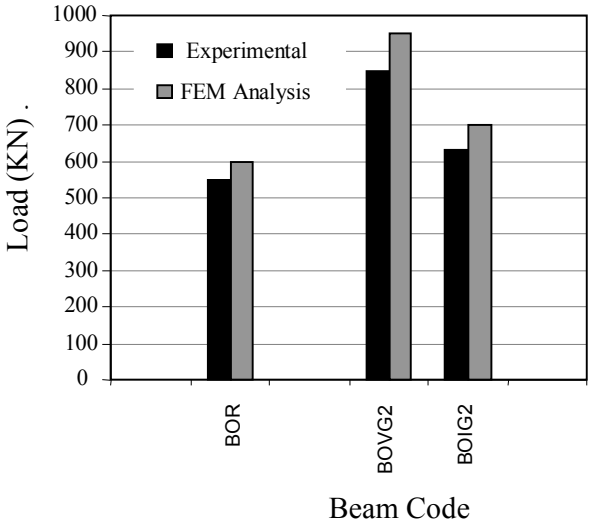

Fig. 24: Expermintal and analytical ultimate failure loads

9. Conclusions

The following conclusions can be drawn from this research work.

1- The new technique suggested in this research work which depends on using intertwined roving NSM GFRP rods saturated with epoxy proved to be efficient for shear strengthening of RSCC deep beams with respect to the traditional methods.

2- In case of strengthening by vertical NSM intertwined roving GFRP rods, anchoring the rods through the web thickness in the transverse direction increases the ultimate load capacity by about 55%.

3- In this study, shear strengthening using NSM reinforcement increases the ultimate load capacity more than the EBL technique when using the same material.

4- Using vertical NSM steel or CFRP strips in transverse direction to the face gives better results than using it in parallel direction.

5- In this study, it was noticed that using NSM vertical reinforcement gives higher capacity than inclined reinforcement, and this may be attributed to the increase of the strengthened area. It is recommended to the increases of the length of the inclined bars to get better results.

6- Isoparametric degenerated layered elements can represent self consolidating concrete, steel reinforcement, different strengthening materials and techniques such as NSM FRP rods or externally bonded FRP layers.

7- The suggested FE model for shear strengthening is quite accurate in representing the problem and the developed FE computer program can be applied to study different cases of strengthening that are not included in the experimental program.

References

[1] Russo, G., Venir, R., and Pauletta, M. Reinforced Concrete Deep Beams-Shear Strength Model and Design Formula. ACI Structural Journal. V.102, No.3, pp. 429-437, May-June, 2005.

[2] Soliman , S.M. Behavior and Analysis of Reinforced Concrete Deep Beams. M.Sc. thesis, Menoufiya University, Egypt, 2003.

[3] Aguilar, G., Matamoros, A.B., Ramirez, J.A., and Wight, J.K. Experimental Evaluation of Design Procedures for Shear Strength of Deep Reinforced Concrete Beams. ACI Structural Journal, V.99, No.4, pp. 539-548, July-August, 2002.

[4] Rogowsky, D.M., and Macgregor. J.G. Shear Strength of Deep Reinforced Concrete Continuous Beams. Structural Engineering Report No. 110. Department of Civil Engineering, University of Alberta, Canada, T6G-276, November, 1983.

[5] Oh, J.K., and Shin, S.W. Shear Strength of Reinforced High-Strength Concrete Deep Beams. ACI Structural Journal, Vol.98, No.2, pp.164-173, March-April, 2001.

[6] Park, J., and Kuchma D. Strut-and-Tie Model Analysis for Strength Prediction of Deep Beams. ACI Structural Journal, Vol.104, No.6, pp.657-666, November-December 2007.

[7] Brown, M.D. and Bayrak, O. Design of Deep Beams Using Strut-and-Tie Models. ACI Structural Journal, V. 105, No. 4, July-August 2008.

[8] Egyptian Code of Practice: ECP 203-2007. Design and Construction for Reinforced Concrete Structures. Ministry of Building Construction, Research Center for Housing, Building and Physical Planning, Cairo, Egypt, 2007.

[9] ACI Committee 318-08. Building Code Requirements for Reinforced Concrete ACI 318-08 and Commentary. American Concrete Institute, Detroit, 2008.

[10] Eurocode 2: DD ENV 1992-1-2-2004. Design of Concrete Structures - Part 1: General Rules and Rules for Buildings. British Standard, BSI, 2004.

[11] Lange, D.A. Struble, L.J., and Dambrosia, M.D. Performance and Acceptance of Self-Consolidating Concrete. Research Report FHWA-ICT-08-020, Illinois Center for Transportation, July, 2008.

[12] Ravindrarajah, S., and Farrokhzadi, F. Properties of Flowing Concrete and Self-Compacting Concrete with High-Performance Superplasticizer. 3rd International RILEM Symposium. Reykjavik, Iceland, 17-20 August, 2003.

[13] Etman, Z.A. Properties and Fields of Application of Self-Compacted Concrete. M.Sc. Thesis, Menoufiya University, Egypt, 2004.

[14] Research Center for Housing, Building and Physical Planning, Cairo, Egypt. Strength of Material and Quality Control Department. State-of-the Art-Report on Self-Compacting Concrete, October. 2002.

[15] Ouchi, M., Nakamura, S.A., Osterberg, T., Hallberg, S.E., and Lwin, M. Applications of Self-Compacting Concrete in Japan. Europe and the United States. I SHPC, 2003.

[16] Okamura, H. and Ouchi, M. Self-Compacting Concrete. Journal Advanced Concrete Technology. Japan Concrete Institute, Vol. 1 , No. 1, April, 2003.

[17] Kiousis, P.D., and Whitcomb, B.L. Study on the Use of Self-Consolidating Concrete for the Repair of the Mead Bridges. Report No. CDOT-2007-1, Interim Report, 2007.

[18] Trent, J.D. Transfer Length, Development Length, Flexural Strength, and Prestress Loss Evaluation in Pre-tensioned Self-Consolidating Concrete members. Master of Science Thesis. Faculty of the Virginia Polytechnic Institute and State University, May, 2007.

[19] Dymond, B.Z. Shear Strength of a PCBT-53 Girder Fabricated with Light-weight, Self-Consolidating Concrete. Master of Science Thesis, Faculty of the Virginia Polytechnic Institute and State University, November, 2007.

[20] Oliva, M.G., and Cramer, S. Self-Consolidating Concrete: Creep and Shrinkage Characteristics. Report to Spancrete County Materials. Department of Civil and Environmental Engineering University of Madison, Wisconsin, Australia. January, 2008.

[21] Heiza, Kh. M., Kamal, M.M., Meleka, N.M. and Elabouky. S. Experimental Study on Repair and Strengthening of Self-Compacted RC Beams. Sixth Alexandria International Conference on Structural and Geotechnical Engineering. Alexandria University, Alexandria, Egypt, 15-17 April, 2007.

[22] Meleka, N.N. Behavior of RC Deep Beams with Openings Strengthened in Shear Using Near Surface Mounted Reinforcement. Civil Engineering Research Magazine, CERM, Al-Azhar University Vol. 29, No. 2 April, 2007.

[23] Rizkalla, S., and Hassan T. Various FRP Strengthening Techniques for Retrofitting Concrete Structures. ICE 2001 Conference Proceedings, Hong Kong; December 2001.

[24] Chen, Z.F. and Wan, L.L. Evaluation of CFRP, GFRP and BFRP Material Systems for the Strengthening of RC Slabs. Journal of Reinforced Plastics and Composites, January, 2008.

[25] Nordin, H., Taljsten, B., and Carolin, A. Concrete Structures Strengthened with Near Surface Mounted Reinforcement of CFRP. Paper B, Licentiate Thesis, Lulea University of Technology, Sweden. 2003.

[26] El-Hacha, R., and Rizkalla, S.H. Near Surface Mounted Fiber Reinforced Polymer Reinforcements for Flexural Strengthening of Concrete Structures. ACI, Structural Journal, Vol.101, No.5, PP.717-726, September-October, 2004.

[27] De Lorenzis, L., Lundgren, K., and Rizzo, A. Anchorage Length of Near-Surface Mounted Fiber Reinforced Polymer Bars for Concrete Strengthening-Experimental Investigation and Numerical Modeling. ACI, Structural Journal, V.101, No.2, PP.269-278, March-April, 2004.

[28] De Lorenzis, L.,and Nanni, A. Shear Strengthening of Reinforced Concrete Beams with Near Surface Mounted Fiber Reinforced Polymer Rods. ACI Structural Journal, V.98, No.1, PP.60-68, January-February, 2001.

[29] Barros, J., Sena, J., Dias, S., Ferreira, D. and Fortes, A. Near Surface Mounted CFRP-Based Technique for the Strengthening of Concrete Structures. Jornada Técnica en Honor a Ravindra Gettu. 5 Octobre, 2004.

[30] El-Wakkad, N. Y. Strengthening of Reinforced Concrete Deep Beams using Near- Surface Mounted Technique (NSM). Ph.D thesis menoufiya university, Egypt 2008.